INTERNATIONAL JOURNAL of PARTICLE THERAPY

Dosimetric Effect of Biozorb Markers for Accelerated Partial Breast Irradiation in Proton Therapy

Melton D. Parham Jr, MS[1]; Salahuddin Ahmad, PhD[2]; Hosang Jin, PhD[2]

[1]Sun Nuclear Cooperation, Melbourne, FL, USA
[2]Department of Radiation Oncology, University of Oklahoma Health Sciences Center, Oklahoma City, OK, USA

Abstract

Purpose: To investigate dosimetric implications of biodegradable Biozorb (BZ) markers for proton accelerated partial breast irradiation (APBI) plans.

Materials and Methods: Six different BZs were placed within in-house breast phantoms to acquire computed tomography (CT) images. A contour correction method with proper mass density overriding for BZ titanium clip and surrounding tissue was applied to minimize inaccuracies found in the CT images in the RayStation planning system. Each breast phantom was irradiated by a monoenergetic proton beam (103.23 MeV and 8×8 cm^2) using a pencil-beam scanning proton therapy system. For a range perturbation study, doses were measured at 5 depths below the breast phantoms by using an ionization chamber and compared to the RayStation calculations with 3 scenarios for the clip density: the density correction method (S1: 1.6 g/cm^3), raw CT (S2), and titanium density (S3: 4.54 g/cm^3). For the local dose perturbation study, the radiographic EDR2 film was placed at 0 and 2 cm below the phantoms and compared to the RayStation calculations. Clinical effects of the perturbations were retrospectively examined with 10 APBI plans for the 3 scenarios (approved by our institutional review board).

Results: In the range perturbation study, the S1 simulation showed a good agreement with the chamber measurements, while excess pullbacks of 1∼2 mm were found in the S2 and S3 simulations. The film study showed local dose shadowing and perturbation by the clips that RayStation could not predict. In the plan study, no significant differences in the plan quality were found among the 3 scenarios. However, substantial range pullbacks were observed for S3.

Conclusion: The density correction method could minimize the dose and range difference between measurement and RayStation prediction. It should be avoided to simply override the known physical density of the BZ clips for treatment planning owing to overestimation of the range pullback.

Keywords: Biozorb; APBI; proton therapy; range perturbation

Introduction

Proton therapy has been proposed as an alternative treatment method for accelerated partial breast irradiation (APBI) owing to reduced dose to critical organs and nontarget breast tissues, improved target coverage, and potential to improve quality of life [1–7]. Protons minimize dose to surrounding healthy tissues and lower exit doses. This means that the breast tissue that surrounds the tumor bed receives a lesser dose, organs-at-risk

Submitted 13 Oct 2020
Accepted 22 Dec 2020
Published 08 Mar 2021

Corresponding Author:
Hosang Jin, PhD
Department of Radiation Oncology
University of Oklahoma Health Sciences Center
800 NE 10th Street, OKCC L100
Oklahoma City, OK 73104, USA
Phone: +1 (405) 271-3016
Fax: +1 (405) 271-8297
hosang-jin@ouhsc.edu

Original Article

DOI
10.14338/IJPT-20-00077.1

http://theijpt.org

such as the heart or lungs receive minimal dose to none, and the probability of secondary cancers is reduced. These benefits are seen in the study of Taghian et al [4], which demonstrated that proton treatment reduced V50 (percent volume receiving 50% of prescribed dose) of nontarget breast tissue by approximately 40% to 45% compared to photon-based treatment. APBI has been proven to benefit from proton therapy but brings also the importance of accurate planning requirements.

A treatment planning system (TPS) uses computed tomography (CT) images to obtain mass density information to calculate the stopping power of the various tissues in the proton's path to the target volume [8]. With the stopping power of tissue known, TPS can calculate the range of a proton beam to correlate the Bragg peak to the depth of the target volume. However, misinformation from the medical images can cause the range of the proton to be perturbed. For example, CT scans can produce image artifacts caused by metal implants that saturate Hounsfield units (HUs) for parts of an image, causing misidentification of correct mass densities of tissues. This in turn results in the wrong determination of proton range. In addition, there is intrinsic inaccuracy of TPS calculation algorithms to predict dose perturbation by metal implants. Jia et al [9] investigated dose perturbation with 2 metallic screw implants (45-mm stainless steel [SS] and 35-mm titanium [Ti]) for spinal cord that presented dose enhancement up to 12% (SS) and 8% (Ti) immediately downstream from the screw in chamber and film measurements but 5% (SS) and 2% (Ti) dose reductions in Eclipse (Varian Medical Systems, Palo Alto, California) TPS. The significant dose discrepancies at the metal-water interface between measurements and the TPS presumably resulted from the secondary electron fluence perturbation whose effect was not accurately modeled in the pencil-beam algorithm. In another study, Giebeler et al [10] found that perturbation of proton dose by implanted gold markers for prostate cancer was 31% for large markers (helix diameter of 1.15 mm) and 23% for medium markers (helix diameter of 0.75 mm) in an oblique orientation using Monte Carlo (MC) simulations. Newhauser et al [11] reported that gold markers used in proton prostate treatment made unacceptably large dose shadows, while Ti and SS markers minimally perturbed the proton beam, using MC simulations.

The Biozorb (BZ; Hologic Inc, Marlborough, Massachusetts) is a 3-dimensional biomarker to improve outcomes in breast-conserving surgery and aid in the treatment of radiation therapy planning by allowing easier and quicker identification of surgical excision sites after removal of malignancy [12, 13]. After removal of tumors via a lumpectomy or mastectomy, it is a common practice to follow the surgery with radiation therapy to ensure that the invasion from microscopic collagens is not allowed in the surrounding tissues. Conventional setup verification using a 2D orthogonal x-ray image pair is difficult for identifying the tumor bed owing to poor soft tissue contrast. The BZ marker consists of bioabsorbable plastic (absorbed by the patient's body over several years) and 6 titanium clips that can easily be identified when imaged by x-ray. Wiens et al [12] concluded that BZ could significantly reduce target volumes for photon therapy.

Although providing quicker identification, this solution engenders many problems for proton therapy. Substantial dose reduction (up to 23%) by the BZ markers was observed for proton therapy in a MC simulation study [14]. In addition, the size and shape of the BZ markers are exaggerated on the CT scan, resulting in incorrect stopping power used in TPS, which leads to differences of the proton range and dose between calculated plan and actual treatment. The purpose of this investigation is to understand the dosimetric effect of different BZs used for proton APBI through empirical measurements and calculations with a commercially available MC-based TPS. This investigation will focus on accurate representation of the titanium clips to reduce CT imaging error, the dosimetric effect of each clip, and the clinical effect of BZ for proton APBI treatment.

Materials and Methods

Biozorb Markers and Breast Phantom

Two different categories of BZs were used in this study: Low Profile (LP) and Spiral (SP) both containing 6 ring-shaped titanium clips (**Figure 1a**). The LP markers (clip size [ring]: 3-mm diameter and 0.9-mm wire width) were smaller than the SP markers (clip size [oval]: 6 mm long and 1-mm wire width). The typical volumes occupied by the LP markers were 6 to 7.1 cm^3, which accommodates women with smaller breasts. Oval (LP1: 2 cm wide $\times$ 3 cm long $\times$ 1 cm thick) and circular (LP2: 3-cm diameter $\times$ 1 cm thick) LP markers were tested in this study. SP markers were all spiral shaped in various sizes. The sizes (diameter $\times$ length in cm) were 2×2 (SP1), 2×3 (SP2), 3×4 (SP3), and 4×4 (SP4). The typical volumes occupied by the SP markers were 4.2 to 33.5 cm^3. This range of volume was much wider than for the LP markers, allowing for the titanium clips to be spaced further apart. The SP markers were preferable for larger tumor cavities and more visible on the x-ray images.

To simulate clinical planning with the BZs, the markers were placed into TX Products solidifying powder (Oil Center Research LLC, Lafayette, Louisiana). The solidifying powder once combined with water created a pink gelatin mold surrounding each marker, mimicking breast tissue. During placement it was ensured that when solidifying, the BZs were

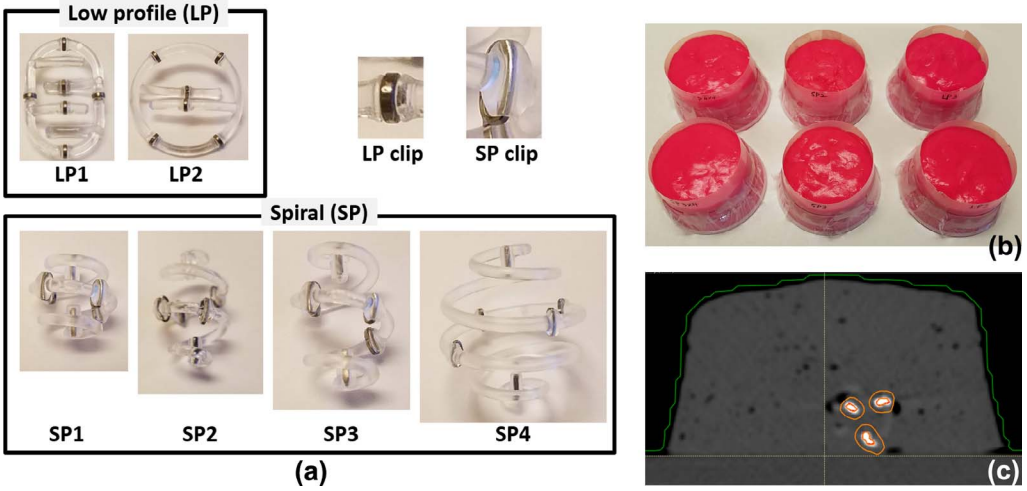

Figure 1. Biozorb markers and breast phantoms. (a) Six Biozorb markers and clips: LP1: 3 cm long × 2 cm wide, LP2: 3-cm diameter, SP1: 2-cm diameter × 2 cm long, SP2: 2-cm diameter × 3 cm long, SP3: 3-cm diameter × 4 cm long, and SP4: 4-cm diameter × 4 cm long; (b) 6 phantoms with the markers inserted at the bottom of the phantom; and (c) axial view of CT scan for the SP1 phantom with titanium clip (center) and soft tissue (ring shape) contours.

placed toward the bottom of the phantom, which was about 5 cm thick considering a typical target depth and 10-cm diameter (**Figure 1b**). The breast phantoms were scanned by a GE Discovery (Chicago, Illinois) CT scanner with 120 kVp, 16 slices, 2.5-mm slice thickness, 0.7-mm pixel, and helical setup (our standard breast scanning protocol). **Figure 1c** shows an axial CT slice of SP1. With each CT image obtained, it was observed that each image contained inaccuracy of titanium clip's size, shape, and HU. In general, the clip size was larger on the CT images than the physical size and center holes of the clips were not visible. This issue was found to be partly correlated with the 2.5-mm slice thickness. The CT reconstruction with the slice thickness made the titanium clips larger by 1 to 2 mm in width and 1 to 4 mm in length and smeared the detailed clip structure. Another issue was saturation of HU value for the titanium clips owing to 12-bit CT image (dynamic HU range from −1000 to 3071). The physical density of titanium (∼4.54 g/cm^3) was much higher than the range of the HU-to-mass density calibration curve for the CT scanner (3071 for maximum density of 2.8 g/cm^3 for our GE system). The saturation occurred only for the SP markers whose clips were relatively larger. The small LP clips did not show the saturation even if the material was titanium. This effect resulted not only in the clip being misrepresented, but also in surrounding tissue having an increase in HU.

Range Perturbation Study

A parallel plate ionization chamber (PPC05, IBA Dosimetry, Schwarzenbruck, Germany) was selected to measure perturbation of the proton range caused by the BZ markers. A diameter of the collecting electrode was about 1 cm. The 2 phantoms (SP1 and SP2) were selected owing to compactness of the titanium clips allowing multiple clips to be present within the active area of the chamber during irradiation. The phantoms were placed on 8 cm of solid water for the CT scan. An 8×8-cm^2 proton beam (1089 spots, 2.5-mm spot spacing, air gap of ∼5 cm, and 1.5 monitor unit/spot) was delivered to the phantoms by using the Mevion (Littleton, Massachusetts) S250i pencil-beam scanning proton therapy system. The dose was 227 cGy at 5-cm depth and 490 cGy at the Bragg peak. The energy of 103.23 MeV (a nominal range [distal 90%] of 8.07 g/cm^2) was selected by examining typical distal APBI energies. Lower-energy proton beams were not generally perturbed by the BZ markers (ie, shallower than the BZ depth). Doses were measured at 0.16-, 2.16-, 2.66-, 3.16-, and 3.66-cm depth below the breast phantoms with and without the titanium clips with consideration of inherent water-equivalent thickness of the PPC05 (0.16 g/cm^2) to determine the range perturbation.

The PPC05 chamber measurements were performed at least twice and the average dose was converted to relative biological effectiveness (RBE)–weighted dose by multiplying with 1.1. The chamber measurements were simulated with the RayStation (RaySearch Laboratories, Stockholm, Sweden) MC calculations (version 9A). In RayStation, 38 regions of interest (1-mm resolution in the Bragg peak region and 5 mm elsewhere) that mimicked the active volume of the PPC05 ion chamber (1-cm diameter and 0.6 mm high) were made and the average doses in cGy (RBE) of the regions of interest were calculated to create depth dose curves for the chamber measurements. By the comparison without the titanium clips, the inherent range differences between chamber measurements and RayStation calculations were found. The range perturbation by the clips was determined by comparing the chamber measurement with the clips to the RayStation simulation, considering the inherent range difference.

Table 1. Patient list for APBI clinical study.

Patient ID	CTV, cm^3	Tumor bed location	Gantry angles, degree	Biozorb
1	53.7	Left	0, 100	SP1
2	30.9	Left	0, 90	LP2
3	58.5	Left	20, 60	SP2
4	133.5	Left	0, 90	SP4
5	48.9	Left	0, 90	SP1
6	57.2	Right	20, 70	SP2
7	109.9	Right	0, 90	SP3
8	51.3	Right	10, 60	SP1
9	97.1	Right	20, 90	SP3
10	173.2	Right	20, 90	SP4

Abbreviations: SP, Spiral; LP, Low Profile.

To mitigate the range perturbation by BZ in RayStation, proper contouring of the titanium clip was investigated. This was done to better represent the realistic shape and size of the BZ marker with a proper mass density. First, the titanium clips were contoured on the basis of HU values higher than surrounding tissue ($>\sim$500). Next, the titanium clip contour was uniformly contracted by 0.5 mm in 3-dimensional space and was assigned to be the titanium clip (it made the clip contour close to the physical size). And then a 2-mm uniform expansion, based on the titanium clip contoured, was performed and assigned to be a temporary tissue. Subtracting the clip contour from the temporary tissue provided a more accurate representation of the surrounding soft tissue as shown in **Figure 1c**. The tissue contour was manually edited to exclude unintended air pockets in the phantoms. The proper mass density of the soft tissue contour was assigned by taking an average mass density of the surrounding tissue. This resulted in a mass density of 1.04 g/cm^3 for the phantom material. The realistic mass density for the clip contour to give the best match between chamber measurement and TPS simulation could be found by changing the mass density with various materials in RayStation. In this study, a bone-based mass density of 1.60 g/cm^3 showed the optimal result (scenario 1). For comparison, the RayStation simulations with the raw CT images (scenario 2: no mass density overridden) and a default RayStation titanium density (4.54 g/cm^3) for the clip contour (scenario 3) were performed. The dose grid size of the RayStation computation was $1\times1\times1$ mm^3 for the phantom study.

Dose Perturbation Study

Although the range perturbation was observed by the group of clips, the active area of the chamber was too large to detect dose perturbation by each titanium clip. The radiographic EDR2 film (Carestream Health, Rochester, New York) was selected to measure the local dose shadowing effect by the clips. Similar to the PPC05 setup, solid water blocks were put underneath each breast phantom to be irradiated by the Mevion S250i system. Below the phantom, 2 sheets of EDR2 film were placed at depths of 0 cm (252 cGy (RBE)) and 2 cm (380 cGy (RBE)), respectively. Four fiducial pinpricks were made with room lasers for image registration. The film sheets were irradiated by the 8×8-cm^2 proton beam for the 6 BZ phantoms. A sheet of film was irradiated with varying levels of known doses (0-400 cGy) to create an optical-density to dose relationship for the measurements. All processed film sheets were scanned with EPSON 10,000XL (Nagano, Japan) scanner in 150 dpi. The planar doses at the corresponding depths (0 and 2 cm below the phantom) extracted from the RayStation simulations were compared with the film measurements by using an in-house Matlab (MathWorks, Natick, Massachusetts) code. The RayStation simulation was performed with the raw CT scan and the clip contour correction (clip density $=$ 1.6 g/cm^3 and soft tissue density $=$ 1.04 g/cm^3). Both film and calculation image sizes were rescaled to 0.5 mm/pixel to compare.

Clinical Simulation Study

Ten APBI treatment plans were retrospectively selected to test the effect of the clip contour correction in clinical planning. This study was approved by the institutional review board of the University of Oklahoma Health Sciences Center. **Table 1** presents a summary of the patient list. The clip and tissue contour were created as described in the previous section (scenario 1) and the mass densities for the clip and tissue contours were overridden with 1.6 g/cm^3 and 1.0 g/cm^3 (average density of the tumor cavity), respectively. Each APBI treatment was prescribed the dose of 30 cGy (RBE) in 5 fractions. The plans were generated

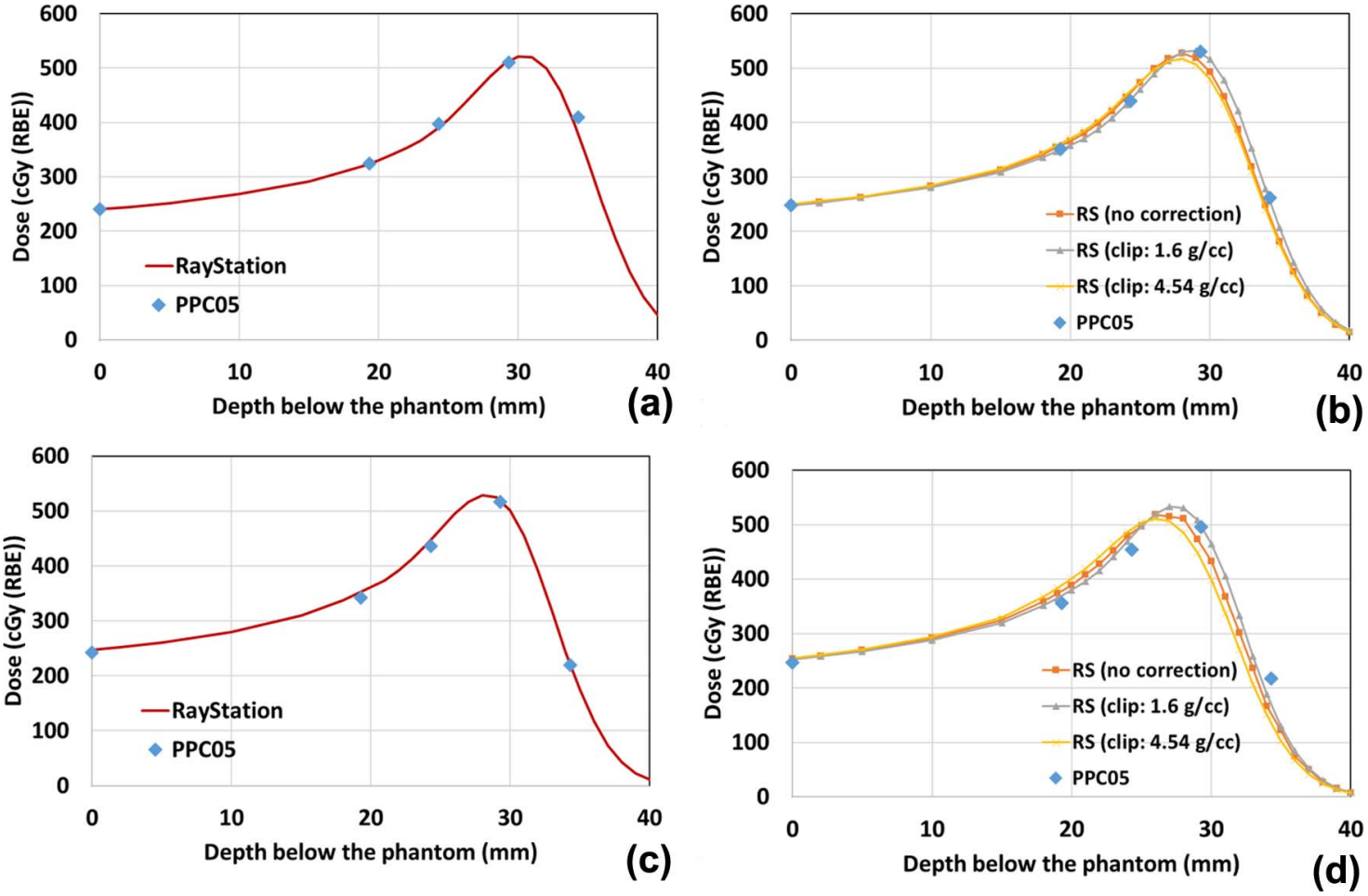

Figure 2. Chamber measurements shifted left by 1.3 mm for the optimal matching compared with RayStation calculations. Measurements for SP1 (a) without and (b) with clips, and SP2 (c) without and (d) with clips. Abbreviation: RS, RayStation.

with 2 beams, single-field optimization with 1-cm block margin, and robust planning (5-mm setup uncertainty and 3.5% range uncertainty) in RayStation. The calculation grid size clinically used was 2×2×2 mm^3. The dose was normalized to ensure 99% of the clinical target volume (CTV) was covered by the prescription. The plans were then recalculated on the raw CT images without any density correction and with the clip contour overridden with the default titanium density (4.54 g/cm^3) to compare. The plans were evaluated by comparing target coverage, ipsilateral lung dose, ipsilateral breast dose, and heart dose in terms of D_{mean} (mean dose) and D_{max} (maximum dose).

Results

Range Perturbation Study

The PPC05 chamber measurements without the titanium clips showed a good agreement with the RayStation calculations with a systematic shift of 1.3 mm (the measurements were deeper) from the nominal depths for both SP1 and SP2 markers as shown in **Figure 2a** and **2c** (the shift applied). The shift might stem from uncertainties in the chamber setup, mass density of solid water blocks and the chamber front window, and range of the energy as compared with the RayStation TPS. **Figure 2** shows comparison between the chamber measurements with the clips and the 3 different RayStation simulations. The chamber measurements were also shifted by 1.3 mm. Among the 3 scenarios, the scenario 1 (clip density: 1.6 g/cm^3) showed the best match with the chamber measurements. In the scenario 2 (no correction) and scenario 3 (clip density: 4.54 g/cm^3), range pullbacks of 1 to 2 mm were observed. Especially, a noticeable peak dose reduction was found in scenario 3.

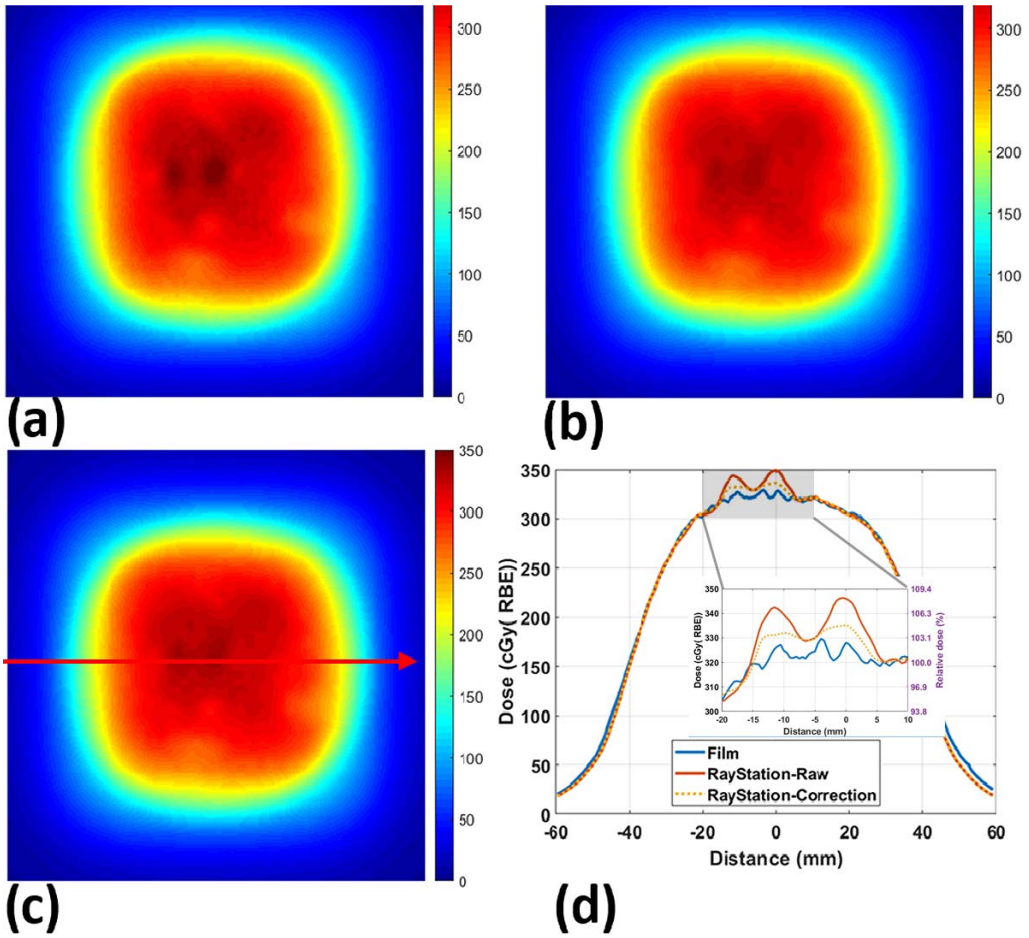

Figure 3. Dose comparison between EDR2 film measurement and RayStation simulation: (a) RayStation with raw CT, (b) RayStation with density correction, (c) EDR2 film measurement, and (d) profiles along the scanline in (c). Abbreviation: CT, computed tomography.

Dose Shadowing Study

If the titanium clips pull back the proton range of the monoenergetic beam, dose under the clips before the Bragg peak is usually higher than the surrounding area. However, the high-resolution film measurements revealed local underdosing under the clips due to depletion of protons by scattering, which could not be seen in RayStation. **Figure 3** shows this local dose shadowing in the film measurement for SP2 at 2-cm depth (small ripples in the film profile in **Figure 3d**). The maximum shadowing compared to surrounding dose level was about –4.0% for the SP clips. RayStation simulations (**Figure 3a** and **3b**) could only predict the higher dose by the range pullback under the clips and could not accurately predict the local dose shadowing effect even with the 1-mm dose calculation grid. Note that the RayStation calculation with the density correction presented a better agreement with the film measurement than that without correction (**Figure 3d**).

The dose difference between film and RayStation for each clip without and with the density correction was observed. **Table 2** shows the maximum, the minimum, and the average dose difference of the 6 titanium clips for each phantom. Negative values indicate that the film measurements were lower than the RayStation simulations. For SP2 and SP3, 2 abutting clips could not be resolved on the film measurements at 2-cm depth; therefore only 4 clip structures were analyzed. In general, these overlapping clips from the delivery angle made the dose difference higher. The SP markers had a higher level of perturbation than the LP markers especially at 2-cm depth, and the dose perturbation was higher at the deeper depth. Improvement of the RayStation dose prediction by the density correction was limited for LP markers and shallow depth (less than 1%); however, it was pronounced at deeper depth with the larger SP clips, especially when the overlapping clips existed (up to 5.5% for SP2).

Clinical Study

Figure 4 shows dose comparison for patient 1 treated with APBI. No substantial difference among the 3 plans was observed in terms of target coverage and dose to normal tissues as shown in **Figure 4f**. The difference in D_{mean} of the structures for 3

Table 2. Dose difference under the 6 clips between film (F) and RayStation (RS) calculation ([F–RS]/background dose × 100%).

	Maximum error, %		Minimum error, %		Average, %	
Marker	**Raw CT**	**Density correction**	**Raw CT**	**Density correction**	**Raw**	**Density correction**
0-cm depth						
LP1	−5.4	−5.1	−0.6	0.7	−3.4	−2.8
LP2	−6.1	−5.8	−3.0	−2.2	−5.1	−4.8
SP1	−5.8	−4.0	−3.4	−2.2	−4.4	−3.2
SP2	−3.8	−2.7	−2.1	−0.3	−3.1	−1.6
SP3	−4.3	−3.6	−1.6	−1.3	−3.1	−2.7
SP4	−7.2	−5.6	−2.2	−2.0	−4.4	−4.1
2-cm depth						
LP1	−4.8	−3.8	−2.3	−1.6	−3.7	−2.7
LP2	−6.4	−5.4	−3.1	−2.6	−4.9	−4.1
SP1	−10.3	−7.8	−7.7	−4.3	−9.4	−6.7
SP2	−10.9	−5.4	−4.4	−2.6	−7.0	−3.9
SP3	−12.8	−8.2	−5.2	−3.6	−7.9	−5.5
SP4	−7.2	−7.0	−0.5	−0.5	−4.2	−3.6

Abbreviations: CT, computed tomography; LP, Low Profile; SP, Spiral.

scenarios of 10 plans compared was negligible (all less than 2 cGy (RBE); 0.1% prescription). The maximum differences in D_{max} between scenario 1 (correction) and scenario 2 (raw CT) for CTV, ipsilateral lung, ipsilateral breast, and heart were 0.4% (patient 4), 1.5% (patient 1), 0.4% (patient 4), and 0.1% (patient 10), respectively. Those between scenario 1 and scenario 3 (Ti density) were 0.6% (patient 7), 1.5% (patient 1), 0.6% (patient 7), and 0.2% (patient 5), respectively. The dose difference

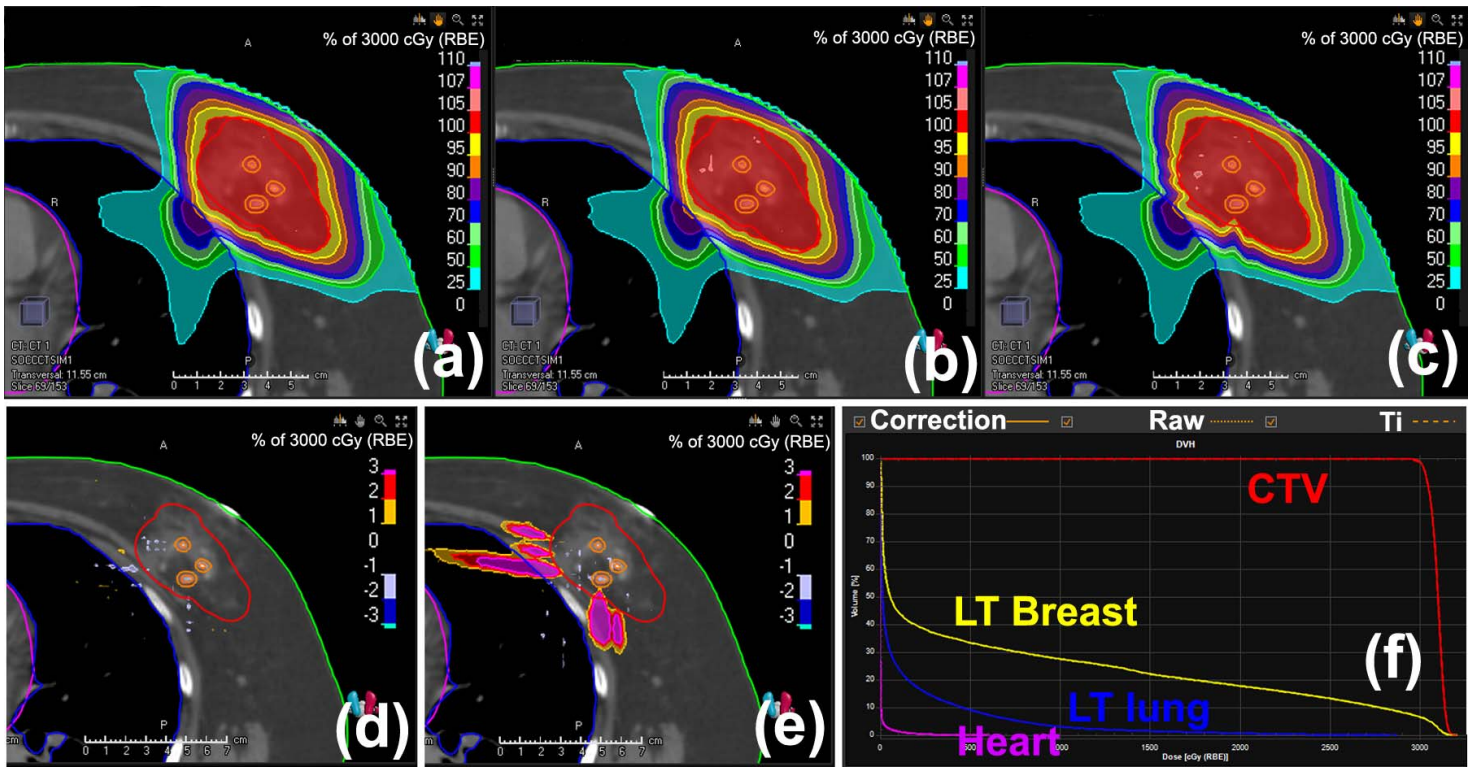

Figure 4. Comparison of APBI plans for patient 1: (a) original plan with density correction; (b) recalculation with the raw CT; (c) recalculation with Ti density for clips; (d) dose difference between (a) and (b); (e) dose difference between (a) and (c); and (f) DVH comparison (solid line: density correction; dotted line: raw CT; dashed line: Ti density—almost identical for all structures). Abbreviations: APBI, accelerated partial breast irradiation; CT, computed tomography; CTV, clinical target volume; DVH, dose volume histogram; LT, left; Ti, titanium.

map between scenario 1 and scenario 2 also shows negligible local dose perturbation (**Figure 4d**). However, noticeable local dose perturbation and range pullback were observed by overriding the Ti density (**Figure 4e**). The dose perturbation was mainly at the distal falloff of high-energy beams outside of the target.

Discussion

In a common practice of proton therapy planning, physical mass densities of implant materials are manually assigned when the CT number is saturated. In this study, we found that, when small implanted markers are used, overriding an actual physical mass density can overestimate (or potentially underestimate for other types of markers) range pullback of proton beams. The chamber study revealed that simply overriding the titanium density on the BZ clip could pull back the range by 2 mm or more and lower the peak dose by 4% in the RayStation computation for the energy used. This is mainly because the CT scanners do not have enough resolution to accurately represent the size and detailed structure of the small implanted markers. The titanium clips saturate the CT images, causing the clips to have a lower density than physical density (especially for the 12-bit scanner), exaggerated size, and metal artifact in the surrounding regions.

We proposed the contour correction method to better represent the actual size of the BZ clip with correction of artifact for surrounding tissues. More suitable mass density for the clip was empirically found rather than using the vendor-provided density. This improved the agreement between measurement and TPS prediction. However, the density values provided in this study should be carefully examined for other systems, since these values are dependent upon commissioning of TPS and CT scan parameters. The methodology established in this report can provide a guideline on how to accurately acquire the value. Even with the correction method, the improvement was not dramatic for smaller LP clips and within short distance from the clips. However, the correction method substantially improved the agreement as the distance from the clips increased and the clips became larger including overlapping (the maximum error reduction up to 5.5% [SP2] as in **Table 2**). The dose perturbation also depended on the orientation of the clips with respect to the beam direction even if it was not fully quantified owing to difficulty in detecting clip angles. The image artifact can be reduced by a metal artifact reduction (MAR) algorithm; however, it does not accurately represent the detailed structure of the small clip and mass density as well. Jia et al [9] showed that significant dose discrepancies between measurements and the TPS were present even with the MAR CT scans.

The film study revealed that there was distinct dose shadowing (local underdosing) by the clips that was not accurately predicted by the RayStation TPS. This study was originally performed with Gafchromic EBT3 (Ashland, Wilmington, Delaware) but we failed to detect the dose shadowing owing to poor signal to noise ratio of the film. The clips made 3%∼4% cold regions compared to surrounding dose, which made the dosimetric error of up to 12% when compared to RayStation in conjunction with overestimation of dose by range pullback.

The density correction did not play a significant role in improving the plan quality in the clinical study. There was no substantial difference between the plans with and without density correction in terms of target coverage. It is probably because all of the energies whose peak depths were deeper than the clip depth were systematically affected by the range perturbation. The deeper Bragg peaks were thus systematically shifted proximally by the clips so the local dose perturbation was not as pronounced as that in the monoenergy experiment. On the other hand, it was partly because 2 beams were used to make the proton plans. Adding additional beams can reduce this error by ensuring a smaller dose is perturbed by the BZ clips for each beam. A careful selection of beam orientation to avoid one clip in succession of another from the delivery angle can be another solution. However, the potential risk of dose shadowing (**Figure 4e**) should be considered when the BZ markers are used. The range and dose perturbation predicted in the phantom study may overestimate the perturbation in patients, which involves the involuntary range mixing caused by more heterogeneous patient anatomy and the intentional range mixing produced by the common clinical beam angle arrangement.

Ideally, the dose perturbation study should be investigated by using a clinical beam with multiple energy layers such as spread-out Bragg peak. Without the properly known mass density of the clips for accurate dose calculation, it was not easy to make error-free pencil-beam scanning plans (inverse planning). The single energy layer was thus used in this study. The beam energy was carefully selected by examining existing APBI proton plans to represent an energy that could be greatly affected by the BZs. It also simplified an issue of quenching (underresponse of detector at the Bragg peak due to high linear energy transfer) for the film measurement by avoiding superimposing multiple Bragg peaks at the measured depths [15]. A range shifter for shallow targets generally makes larger spots and may contain more low-energy scattered protons. It is believed the overall effect of the larger spots will be limited because the average energy of proton at the marker depth will be similar for different target depths.

Conclusion

In proton APBI cases, caution should be taken if APBI uses BZ markers. The implanted markers cause the underdose effect within the target region and the ''comet tail'' effect (excessive local range pullback) at the distal fall-off regions (usually lung and rib) even though the 2 uniform fields with robust optimization have been implemented. The BZ markers can produce 1- to 2-mm range difference and up to 12% dose error of proton delivery compared to TPS calculation if the markers are not properly handled during planning. A correction procedure, such as the one presented in this report, should be used to minimize this error. Dose shadowing will not be present in TPS owing to limitation of CT imaging and resolution of TPS. The proposed correction method, even if not complete reduction, has a potential to mitigate this error. It should be carefully examined the simple mass density overriding of titanium BZ clips with known titanium density, as this will produce a stronger pullback in TPS than actual delivery.

ADDITIONAL INFORMATION AND DECLARATIONS

Melton D. Parham Jr, MS, contributed excerpts from his master's thesis manuscript, *Dosimetric Investigation of Compact Proton Pencil-Beam Scanning Therapy System for Lung and Breast Cancer* (Oklahoma City, OK: The University of Oklahoma Health Science Center; 2020), for this article.

Conflicts of Interest: The authors have no relevant conflicts of interest to disclose.

Funding: The authors have no funding to disclose.

Ethical Approval: All patient data have been collected under internal review board (IRB)–approved protocol.

References

1. Corbin KS, Mutter RW. Proton therapy for breast cancer: progress & pitfalls. *Breast Cancer Manag*. 2018;7:BMT06.
2. Ovalle V, Strom EA, Shaitelman S, Hoffman K, Amos R, Perkins G, Tereffe W, Smith BD, Stauder M, Woodward W. Proton partial breast irradiation: detailed description of acute clinico-radiologic effects. *Cancers (Basel)*. 2018;10:111.
3. Kozak KR, Smith BL, Adams J, Kornmehl E, Katz A, Gadd M, Specht M, Hughes K, Gioioso V, Lu H-M, Braaten K, Recht A, Powell SN, DeLaney TF, Taghian AG. Accelerated partial-breast irradiation using proton beams: initial clinical experience. *Int J Radiat Oncol Biol Phys*. 2006;66:691–8.
4. Taghian AG, Kozak KR, Katz A, Adams J, Lu H-M, Powell SN, DeLaney TF. Accelerated partial breast irradiation using proton beams: initial dosimetric experience. *Int J Radiat Oncol Biol Phys*. 2006;65:1404–10.
5. Shaitelman SF, Kim LH. Accelerated partial-breast irradiation: the current state of our knowledge. *Oncology*. 2013;27:329–42.
6. Mutter RW, Jethwa KR, Gonuguntla K, Remmes NB, Whitaker TJ, Hieken TJ, Ruddy KJ, McGee LA, Corbin kS, Park SS. 3 fraction pencil-beam scanning proton accelerated partial breast irradiation: early provider and patient reported outcomes of a novel regimen. *Radiat Oncol*. 2019;14:211.
7. Wang X, Zhang X, Li X, Amos RA, Shaitelman SF, Hoffman K, Howell R, Salehpour M, Zhang SX, Sun TL, Smith B, Tereffe W, Perkins GH, Buchholz TA, Strom EA, Woodward WA. Accelerated partial-breast irradiation using intensity-modulated proton radiotherapy: do uncertainties outweigh potential benefits? *Br J Radiol*. 2013;86:20130176.
8. RaySearch Laboratories AB. *RayStation 8B Reference Manual*. Stockholm, Sweden: RaySearch Laboratories AB; 2018.
9. Jia Y, Zhao L, Cheng C, McDonald MW, Das IJ. Dose perturbation effect of metallic spinal implants in proton beam therapy. *J Appl Clin Med Phys*. 2015;16:333–43.
10. Giebeler A, Fontenot J, Balter P, Ciangaru G, Zhu R, Newhauser W. Dose perturbations from implanted helical gold markers in proton therapy of prostate cancer. *J Appl Clin Med Phys*. 2009;10:2875.
11. Newhauser W, Fontenot J, Koch N, Dong L, Lee A, Zheng Y, Waters L, Mohan R. Monte Carlo simulations of the dosimetric impact of radiopaque fiducial markers for proton radiotherapy of the prostate. *Phys Med Biol*. 2007;52:2937–52.
12. Wiens N, Torp L, Wolff B, Wert Y, Barton K, Weksberg D, Wilson-Dagar J. Effect of BioZorb® surgical marker placement on post-operative radiation boost target volume. *J Radiat Oncol*. 2018;7:175–9.
13. Srour MK, Chung A. Utilization of BioZorb implantable device in breast-conserving surgery. *Breast J*. 2019;26:960–5.

14. Zhang M, Goyal S, Zou W, Yue NJ. Performance evaluation of BioZorb markers in proton therapy for partial breast irradiation. Presented at: 55th Annual Meeting for the Particle Therapy Cooperative Group (PTCOG); 2016; Prague, Czech Republic.
15. Yeo IJ, Teran A, Ghebremedhin A, Johnson M, Patyal B. Radiographic film dosimetry of proton beams for depth-dose constancy check and beam profile measurement. *J Appl Clin Med Phys*. 2015;16:5402.